Fermilab Library
0 1160 0032534 4

LYCEN/9402
January 1994

HYDROGEN ON $Pt_{0.5}Ni_{0.5}$ (110), ALLOYING EFFECTS UPON ADSORPTION.

M. Fallavier, M. Benmansour, B. Hjörvarsson[1] and J.P. Thomas.

Institut de Physique Nucléaire de LYON, IN2P3-CNRS / Université Claude Bernard LYON I
43 Bd du 11 Novembre 1918, F - 69622 Villeurbanne Cedex, FRANCE.

M. Abon, H.A. Atli and J.C. Bertolini.

Institut de Recherche sur la Catalyse, CNRS, conventionné à l'Université Claude Bernard Lyon I, F - 69626 Villeurbanne Cedex, FRANCE.

FERMILAB
JUN 8 1994
LIBRARY

ABSTRACT:

Hydrogen adsorption on $Pt_{0.5}Ni_{0.5}$ (110) was investigated by NRA, TPD, and $\Delta\Phi$ measurements. The crystal surface was characterised by LEED and AES. No reconstruction of the surface was observed upon hydrogen exposure and the initial surface composition remains unaffected. At low temperatures and for hydrogen pressure higher than 10^{-5} mbar, the saturation coverage was found to be close to one monolayer. Under these conditions, the adsorbed hydrogen gives rise to a +600 meV shift in the work function. Up to 0.1 in coverage the initial sticking coefficient (S_0) is 0.1 and the heat of adsorption was found to be 70 kJ/mol. These results are discussed in relation with the structure and composition of the surface and compared to known data for hydrogen adsorption on Ni (110). An interpretation based on the existence of two different adsorption sites is proposed.

1 : Permanent address: Department of Physics, Uppsala University, Uppsala, Sweden

to appear in Surface Science

1. INTRODUCTION.

The surface properties of the transition metal alloys have caused an enhanced interest for model studies on single crystal alloys. Examples of this are the PtNi (111) and (110) single crystal surfaces, on which the surface composition [1-11], chemisorption and catalytic properties [11-15] have been extensively studied. Whereas the surface of $Pt_{0.5}Ni_{0.5}$ (111) is Pt enriched [1-9], the surface of $Pt_{0.5}Ni_{0.5}$ (110) is characterised by a strong Ni surface segregation, as shown by LEED [10] and AES [11] experiments. Furthermore, there is a variation in the composition of the first three atomic layers, with a near-surface interplane relaxation [10].

There are differences in the hydrogen adsorption on Pt and Ni single crystals (for a review, see e.g. [16]). The largest differences are found on the open (110) faces, the H-heat of adsorption is almost 20% larger for the Ni (110) compared to Pt (110). The initial sticking coefficient is close to 1 on Ni (110) [18] compared to about 0.5 on Pt (110) [17]. The clean Pt (110) surface is (1 x 2) reconstructed and remains so under hydrogen adsorption [17], but Ni (110) reconstructs upon hydrogen exposure [19-21]. The hydrogen adsorption on $Pt_{0.5}Ni_{0.5}$ (110) is therefore expected to reveal interesting kinetic and thermodynamic properties due to the complex surface composition. Our investigations are furthermore motivated by the enhanced catalytic activity of this PtNi alloy in the selective hydrogenation of butadiene to butene [11], as one of the key parameters is the hydrogen uptake of the surface.

Various experimental techniques were used in this work: Nuclear Reaction Analysis (NRA), Temperature Programmed Desorption (TPD) and work function measurements ($\Delta\Phi$). The surface characterisation was obtained by low energy electron diffraction (LEED) and Auger Electron Spectroscopy (AES). The characteristics of hydrogen adsorption on $Pt_{0.5}Ni_{0.5}$ (110) obtained in this study are compared to known data for hydrogen adsorption on Ni (110) and discussed taking into account the structure and the composition of the surface.

2. EXPERIMENTAL.

Hydrogen coverage measurements by Nuclear Reaction Analysis (NRA) were performed in a UHV system connected to a beam line of the 4 MV Van de Graaff accelerator at IPNL [22]. The experimental set-up includes sputtering ion gun, electron bombardment heating stage (300-1500 K), Auger Electron Spectroscopy (AES), quadrupole mass spectrometer, and a combined resistive heating and liquid nitrogen cooling stage (115 - 600 K). The coverage measurements were performed using the 6.4 MeV resonance of the $^{1}H(^{15}N,\alpha\gamma)^{12}C$ nuclear reaction. The beam intensity was typically 60 nA and the beam size about 1.5 mm^2. The accuracy of the measurements is better than 10%, and the precision which is determined by the number of detected γ-quanta is generally better than few percents. In the actual experimental conditions, the detection limit was 8.0 10^{13} H at/cm^2. The experimental and calibration procedures are described in detail in previous publications [22,23]. Hydrogen concentrations were measured in presence of the H_2 gas phase. Each measurement requires about one minute of acquisition time. For given pressure and temperature conditions, several measurements are performed at different spots on the crystal surface. This allows to control surface homogeneity, reproducibility and that the saturation concentration is already obtained.

The Temperature Programmed Desorption (TPD), work function changes ($\Delta\Phi$) and Low Energy Electron Diffraction (LEED) measurements were performed in a separate experimental set-up, which has been previously described [24]. Work function changes ($\Delta\Phi$) were measured according to the diode method, using the LEED gun as an electron source. In the TPD experiments, the crystal was resistively heated. The heating rate was approximately 10 K/s. The temperature was measured with a thermocouple, directly spot welded to the crystal edge. As CO is the main source of spurious adsorption on the surface, masses 2 and 28 were simultaneously recorded in order to verify the absence of a significant CO contamination of the surface. We have also checked that no H_2O desorption occured at mass 18.

The procedures for the preparation of the (110) oriented $Pt_{0.5}Ni_{0.5}$ single crystal are found in ref. [10,11]. The same crystal was used in all the experiments. The final cleaning process

consisted of several cycles of Ar^+ ion sputtering, thermal treatment under low oxygen pressure to remove carbon (typically 2 x 10^{-8} mbar of O_2 for 2 minutes at 1000 K) and high temperature annealing (>1100 K). The surface cleanliness was monitored by AES in all performed experiments. The pressure values indicated in the text and in the figures are corrected for the H_2 sensitivity factor of the gauge and of the mass spectrometer.

3. RESULTS.

3.1. Surface characterisation

The high temperature annealing of the $Pt_{0.5}Ni_{0.5}$ (110) crystal in UHV leads to a stable surface composition [11]. The segregation profile has been determined previously by Gauthier et al [10] using the same sample and their results are summarised in Table 1. The first atomic plane consists exclusively of Ni atoms, and the second atomic plane is dominated by Pt (95±4 at. %). We found that the $Pt_{0.5}Ni_{0.5}$ (110) crystal gave rise to a (1x1) LEED pattern, as expected for a non-reconstructed fcc (110) surface, and no change in the (1x1) pattern was observed upon hydrogen exposure. The stability of the surface composition was investigated by an Auger line shape analysis in the range 60-65 eV, as described in ref. [11]. No change in the line shape was observed upon hydrogen exposure. Furthermore, the TPD spectra remained the same for several adsorption-desorption cycles in the temperature range 120 - 400 K and the hydrogen coverage measured by NRA for given temperature and pressure was the same when the crystal was cooled under the H_2 pressure or cooled in UHV before hydrogen exposure. These observations are conclusive evidences for the stability of the $Pt_{0.5}Ni_{0.5}$ (110) surface upon hydrogen exposure. This conclusion is in line with the absence of H-induced segregation in PtNi alloys reported from ISS experiments [25].

3.2. Coverage measurements (NRA).

In figure 1, a selection of isobars is presented. As seen in the figure there are two different domains in temperature. Above 175 K a linear decrease of the coverage with temperature is

observed. Below 175 K the coverage changes more slowly with temperature and even remains constant for the 10^{-7}, 10^{-4} and 5 10^{-4} isobars. The maximum coverage close to one monolayer (1ML = 1.01 10^{15} at/cm^2) was obtained for low temperature adsorption under H_2 pressure higher than 10^{-5} mbar. It corresponds to a saturation level of the hydrogen concentration at 9.2 (± 1.0) 10^{14} at/cm^2 for T ≤ 175 K.

In figure 2, a representative selection of the measured isotherms is presented. Each isotherm results from measurements performed when increasing the pressure in the 10^{-8}-10^{-4} mbar range. Indeed the lower the temperature, the slower the hydrogen desorption. Below room temperature the desorption rate is so low that coverage changes could not be measured in a reasonable time when the H_2 pressure was decreased. The data obtained at given temperature and pressure were comparable, within the error bar of the measurements, to the values measured when decreasing the temperature at a given H_2 pressure. The 115 K isotherm reveals two distinct features. first of all a saturation in the coverage at pressure above 10^{-5} mbar and secondly a non-linear dependence in log(P) for lower pressure. The coverage at the lowest pressure (2 10^{-8} mbar) is 2.2 10^{14} at/cm^2. At higher temperature, the coverage is close to linear in log(P) below the saturation region which is obtained at higher pressure for increasing temperature between 115 and 250 K. At 300 K, no saturation is observed in the coverage, with hydrogen pressure up to 6 10^{-4} mbar. At 250 and 300 K and for a pressure lower than 10^{-7} mbar, the hydrogen concentration measurements did not exceed the experimental background indicating that the coverage was below the detection limit of the NRA technique, i.e. about 0.1 ML.

The isosteric heat of adsorption has been determined from the hydrogen isobars, considering only the domain where the coverage varies with the temperature (T > 175 K) and where the coverage exceeds 0.2 ML (P > 10^{-7} mbar). At low temperature and pressure, the adsorption may not be reversible and therefore the Clausius-Clapeyron equation would not be valid. As reported above, it is difficult to test the thermodynamic reversibility of the measured coverages at low temperature for practical reasons. This behaviour must be considered in connection with the kinetic and thermodynamic informations obtained in these low temperature and pressure ranges from the TPD experiments which are presented and discussed in the

following paragraphs. The various (P,T) values for a given coverage have been obtained by an interpolation procedure between the experimental data points. The values of the isosteric heat of adsorption obtained from the variation of ln(P) versus 1/T at constant coverage, are presented in figure 3. For coverage exceeding approximately 0.5 ML, the isosteric heat of adsorption decreases from 66 ± 5 kJ/mol to 38 ± 5 kJ/mol at Θ_H = 0.8 ML. This can be attributed to H-H repulsive interaction at coverage exceeding 0.5 ML.

Besides the hydrogen coverage, additional information can be obtained from the full width at half maximum (FWHM) of the experimental resonance curve of the $^1H(^{15}N,\alpha\gamma)^{12}C$ nuclear reaction. The total width measured for hydrogen on the $Pt_{0.5}Ni_{0.5}$ (110) surface was 10.8 ± 0.3 keV. This is much larger than the intrinsic resonance width of the nuclear reaction, which is 1.8 keV (Lorentzian shape), and than the width of the initial energy distribution of the beam, which is 3 keV (Gaussian shape). The observed broadening is governed by the vibrational motion of the hydrogen atoms on the surface (i.e. the Doppler effect) [26,27]. The experimental resonance curve is the convolution of the nuclear cross section with the Gaussian distributions of the initial energy distribution and of the Doppler broadening. A Doppler broadening of 9.1 keV has been determined by numerically convoluting the three components of the total width. For a one-dimensionnal harmonic oscillator with zero-point energy E_H, the Doppler width ΔE is

$\Delta E = (16 \ln 2\, E_H\, E_N\, M_N / M_H)^{1/2}$,where E_N is the ^{15}N ion energy of 6.385 MeV and M_N and M_H are the masses of the ^{15}N ion and of the H atom, respectively. The so determined value of E_H is 78 meV. If the broadening would originate from a single vibrational mode perpendicular to the surface plane, it would correspond to an energy transition of 156 meV between the ground state and the first excited state. However, more than one vibrational mode out of the surface plane can have a component in the direction of the surface normal and therefore contribute to the observed broadening of the resonance curve. This situation is highly probable for H atoms adsorbed on a (110) surface as evidenced for H adsorption on Ni (110) in HREELS experiments [20,32]. The FWHM of the resonance that we measured on Ni (110) {(2x1)-H phase} was 11.0 ± 0.3 keV, nearly the same as obtained for the $Pt_{0.5}Ni_{0.5}$ (110) alloy surface. This suggests that hydrogen adsorbs at similar sites on the (110) surface of $Pt_{0.5}Ni_{0.5}$ and Ni.

3.3. TPD measurements.

Adsorption studies were performed with a sample temperature of 120 K under low hydrogen pressure (1.2 10^{-8} mbar). The TPD curves were recorded after a short pumping time (about 30 s), and the pressure was typically in the 10^{-10} mbar range. In figure 4-A, a series of TPD curves is displayed. There is a shift in temperature of the maximum of the desorption rate with increasing hydrogen coverage, which is characteristic of a second order (molecular) desorption. A high temperature shoulder is observed at all coverages and also a low temperature shoulder, which becomes more apparent with increasing coverage. The curves were decomposed into three individual peaks, assuming second-order peak shapes. The decomposition of the TPD spectrum (f) obtained for an exposure of 3.7 10^{-7} mbar.s is shown in fig. 4-B as an example. The temperature corresponding to the maximum of the desorption rate, T_M, decreases with hydrogen coverage from ~ 400 to 380 K for the high temperature (α_3) peak, from ~ 350 to 320 K for the main, medium temperature (α_2) peak, and from ~ 300 to 280 K for the low temperature (α_1) peak. The hydrogen coverage corresponding to the total area under the TDS spectrum at saturation (for large exposures) has been assumed to be equal to the equilibrium concentration of 2.2 10^{14} at./cm^2 measured by NRA for adsorption at the same temperature and pressure. An estimation of the coverage from the integration of the desorption spectrum measured at saturation leads to a value of 1.9 10^{14} at./cm^2 using the measured apparent crystal area (0.95 cm^2) and the measured pumping speed (130 l/s). This value is in good agreement with the concentration measured by NRA. The evolution of the hydrogen coverage as a function of exposure is presented in figure 5 for the three peaks (α_1, α_2 and α_3) as well as the evolution of the total coverage. The area under the α_3 peak is small and saturates at an exposure of less than 0.5 10^{-6} mbar s. The α_1 peak develops with some delay, but contributes then to approximately 30% of the total desorption.

The initial sticking coefficient (S_0), obtained from the TPD measurements, is determined to be 0.1. As shown in figure 6, the sticking coefficient remains constant up to a coverage of 0.1 ML and thereafter it decreases sharply.

The activation energy of desorption (E_D) was determined for the α_2 peak from the TPD results. The peak width analysis developed by Falconer and Schwarz [28] gives $E_D = 70 \pm 7$ kJ/mol. Other methods gave values which fall within this range; The method described by Redhead [29], plotting ln (nT^2_M) versus T^{-1}, gives $E_D = 73$ kJ/mol. The method of King [30] (construction of a family of curves $n = f(t)$ from the original TPD traces) gives for the lowest coverages $E_D = 65$ kJ/mol. The fit with computed desorption traces, as described by Lord and Kittelberger [31], yields E_D in the range 77 to 63 kJ/mol depending on the preexponential factor. An estimation of the desorption energy for the α_3 and the α_1 peak was performed using the differences in the temperature of the maximum rate of desorption compared to the α_2 peak. The resulting energies are 80 kJ/mol for the α_3 peak and 60 kJ/mol for the α_1 peak.

3.4. $\Delta\Phi$ measurements

The adsorption of H_2 (1.2 10^{-8} mbar) on $Pt_{0.5}Ni_{0.5}$ (110) at 120 K, i.e. in the same conditions as the desorption measurements, gives rise to approximately + 300 meV increase in the work function. The changes of $\Delta\Phi$ with exposure are similar to the adsorption kinetics of hydrogen measured by TPD. As shown in Fig. 5, the total hydrogen coverage increases linearly with exposure up to about $\Theta_H = 0.15$ ML. $\Delta\Phi$ scales therefore linearly with the coverage, up to approximately 0.15 ML in coverage. The steady state $\Delta\Phi$ values were measured for H_2 pressures up to 7 10^{-5} mbar, i.e. full coverage. The results are presented in figure 7, all exposures were performed on an initially annealed surface. $\Delta\Phi$ values are shown as a function of the hydrogen coverage, using the results from the NRA measurements. Two distinct domains are observed: a rapid $\Delta\Phi$ increase up to + 300 meV for Θ_H lower than about 0.15 ML, followed by a slower increase from + 300 to + 600 meV.

4. DISCUSSION

As already stated, the top-most layer of the $Pt_{0.5}Ni_{0.5}$ (110) surface exhibits almost solely nickel atoms (see Table 1). Nevertheless, the present work shows that there are significant

differences in the hydrogen adsorption on the alloy compared to Ni (110). The maximum hydrogen coverage is 0.92 ML compared to 1.5 ML for Ni (110) [19,21]. We do not observe any adsorbate induced surface reconstruction, as found for the Ni (110) surface at hydrogen coverages above 1 ML. Furthermore, it is important to note that the maximum coverage of the alloy is only obtained at temperature below 175 K and pressure exceeding 10^{-5} mbar. Conversely on Ni (110) the saturation coverage is obtained at $T \leq 200$ K for low pressure exposures [19 - 21]. The heat of adsorption on the alloy is found to be 70 kJ/mol compared to 90 kJ/mol on Ni (110) [16]. The initial sticking coefficient on the alloy is 0.1 compared to 1 on Ni (110) [18].Moreover the sticking coefficient decreases rapidly for $\Theta_H > 0.1$ ML on the alloy, and is close to 0.01 for $\Theta_H \sim 0.2$ ML, whereas the sticking coefficient on Ni (110) is constant up to $\Theta_H \sim 0.4$ ML. The low hydrogen binding energy and the low sticking coefficient can explain that the hydrogen coverage is reduced on the alloy and that the saturation limit is obtained at higher pressure, compared to the Ni (110) surface.

On an open (110) surface, both the first and the second atomic layers are involved in the hydrogen adsorption. Hydrogen preferentially resides in highly coordinated sites [16]. On the unreconstructed Ni (110) face, on-top sites are not populated [20,21], and the adsorbed atoms occupy inclined quasi threefold sites [32, 33, 34]. Assuming that hydrogen is adsorbed at the same type of sites on the alloy surface, one expects that the Pt enrichment of the second layer will affect the binding energy of hydrogen. A schematic description of the alloy surface is shown in figure 8, indicating possible H adsorption sites. Taking into account the composition of the second atomic layer with about 95 at.% Pt, the most numerous quasi three-fold sites are sites of type I which consist of two Ni atoms in the first layer and one Pt atom in the second layer. The sites of type II are formed by three Ni atoms as on Ni(110), their number should be less than 10% of the quasi three-fold surface sites. Sites of type III are less numerous and can be neglected in the discussion. The structural defects related to vacancies (sites of type IV) contribute to about 3% of the sites (see table 1).

The experimental results can be understood in terms of two different adsorption sites for hydrogen on the surface. By using the mean field approach, adsorption in sites of type I

(2 Ni + 1 Pt atoms) is expected to be less energetically favourable than in sites of type II (3 Ni atoms). This as hydrogen is more strongly adsorbed on Ni than on Pt [16]. Consequently, it may be proposed that the dissociative adsorption of hydrogen requires some activation energy only on sites of type I. The existence of such an activation energy could be an explanation for the rapid decrease of the sticking coefficient above 0.1 ML. Initially the dissociative adsorption of hydrogen will then occur preferentially on sites of type II. Nevertheless, if one assumes a random distribution of sites II on the surface, the dissociative adsorption of H_2 on sites II results in simultaneous filling of sites I. At low temperature and pressure, the direct adsorption on sites of type I would be very limited as suggested by the very low coverage (0.22 ML). The increase of the coverage beyond 0.22 ML for higher pressure, as observed in the NRA and $\Delta\Phi$ experiments, would result from the direct adsorption on sites of type I. This allows to propose the following explanation of the TPD spectra. The α_2 peak could be attributed to the recombination of hydrogen atoms from sites I and II. Following this assumption, the relative area of the α_2 peak (~ 70 % of the total area) can be used to estimate the number of sites II. The maximum coverage measured in the TPD experiments was approximately 0.2 ML, and therefore the number of sites II should be 7% of the total number of sites. This is in agreement with the previously measured surface composition. The α_1 peak, which develops with some delay compared to the α_2 peak, could be attributed to the recombination of hydrogen atoms coming from the same kind of sites, sites of type I. Note that the high temperature α_3 peak, which must correspond to the strongest surface sites, may be related to recombination of H atoms from sites of type II or from structural defects. The experimental uncertainties prevent any conclusive discussion as the coverage relative to the α_3 peak is quite small (< 0.02 ML).

The $\Delta\Phi$ changes with coverage are in agreement with the presence of two different adsorption sites on the surface. At low coverage, the hydrogen induced changes in the work function are dominated by adsorption at sites of type II. The sites of type I are simultaneously populated, but the work function changes associated with population of sites of type II are much larger. Above 0.15 ML in coverage, the changes in the work function are solely due to adsorption at sites of type I. The $\Delta\Phi$ changes on the alloy are positive, as reported for H on Ni (110),

which indicates a net charge transfer from the metal to the hydrogen adatom. Conversely, $\Delta\Phi$ = - 500 meV on Pt (110) at hydrogen saturation [17]. For a given coverage, the change in the work function is larger on the alloy than on Ni (110) where $\Delta\Phi$ = + 245 meV for Θ_H = 1 ML and $\Delta\Phi$ = + 500 meV for Θ_H = 1.5 ML [19]. This observation indicates enhanced charge transfer on the alloy compared to the Ni surface.

5. SUMMARY

Even though the outermost atomic layer consists nearly solely of Ni, the hydrogen adsorption on the $Pt_{0.5}Ni_{0.5}$ (110) surface turns out to be significantly different from hydrogen adsorption on Ni(110). The heat of adsorption of hydrogen on the alloy surface is lower and the sticking coefficient is strongly reduced. The saturation coverage, which is only obtained at relatively high pressure, is close to 1 ML and hydrogen adsorption does not induce a surface reconstruction. As on Ni(110), the positive work function changes indicate a net charge transfer towards the hydrogen atom. The hydrogen induced work function changes are larger on the alloy. As the surface composition is known, the experimental results can be understood in terms of two different H adsorption sites respectively formed by 3 Ni atoms or by 2 Ni + 1 Pt atoms as nearest neighbours. The most numerous sites (2 Ni + 1 Pt) are less energetically favoured and dissociation at these sites probably involves an activation barrier. The catalytic properties of the alloy surface in hydrogenation reactions could be related to the lower binding energy of the H atoms favouring their surface mobility and also to the enhanced negative polarisation of the H atoms.

Acknowledgement

One of us (B.H.), would like to thank the Swedish National Board for Technical Development (STU) for financial support.

REFERENCES

[1] L. de Temmerman, C. Creemers, H. Van Hove, A. Neyens, P. Delichére, J. Massardier, B. Tardy, M. Abon and J.C. Bertolini, Le Vide, Les Couches Minces 38 (1983) 217.

[2] Y. Gauthier, Y. Joly, R. Baudoing and J. Rundgren, Phys. Rev. B31 (1985) 6216.

[3] L. de Temmerman, C. Creemers, H. Van Hove, A. Neyens, J.C. Bertolini and J. Massardier, Surface Sci. 178 (1986) 888.

[4] M. Abon, J.C. Bertolini and H. Montes, Appl. Surface Sci. 32 (1988) 343.

[5] D. Fargues, J.J. Ehrhardt, M. Abon and J.C. Bertolini, Surface Sci. 194 (1988) 149.

[6] J.P. Segaud, E. Blanc, C. Lauroz and R. Baudoing, Surface Sci. 206 (1988) 297.

[7] Y. Jugnet, G. Grenet, N.S. Prakash, Tran Minh Duc and H.C. Poon, Phys. Rev. B38 (1988) 5281.

[8] S. Deckers, F.H.P.M. Habraken, W.F. van der Weg, A.W. Denier van der Gon,B. Pluis, J.F. van der Veen and R. Baudoing, Phys. Rev. B42 (1990) 3253.

[9] E. van de Riet, S. Deckers, F.H.P.M. Habraken and A. Niehaus, Surface Sci. 243 (1991) 49.

[10] Y. Gauthier, R. Baudoing, M. Lundberg and J. Rundgren, Phys. Rev. B35 (1987) 7867.

[11] J.C. Bertolini, J. Massardier, P. Ruiz and B. Tardy, Surface Sci. 211/212 (1989) 1053.

[12] J.C. Bertolini, B. Tardy, M. Abon, J. Billy, P. Delichére and J. Massardier, Surface Sci.135 (1983) 117.

[13] J. Massardier and J.C. Bertolini, J. Catal. 90 (1984) 358.

[14] J. Massardier, B. Tardy, P. Delichére, M. Abon and J.C. Bertolini, Proc. 8th Intern. Congr. on Catalysis, Berlin, (1984) IV-185.

[15] M. Abon, J. Massardier, B. Tardy and J.C. Bertolini, Surface Sci. 189/190 (1987) 880.

[16] K. Christmann, in: Hydrogen Effect in Catalysis, Eds. Z. Paal and G. Menon (Marcel Dekker, New York) (1988) 3; K. Christmann, Interaction of hydrogen with solid surfaces, Surface Sci. Rpts 9 (1988) 1.

[17] J.R. Engstrom, W. Tsai and W.H. Weinberg, J. Chem. Phys. 87 (1987) 3104.

[18] A. Winkler and K.D. Rendulic, Surface Sci. 118 (1982) 19.

[19] K. Christmann, F. Chehab, V. Penka and G. Ertl, Surface Sci. 152/153 (1985) 356.

[20] M. Jo, M. Onchi and M. Nishijima, Surface Sci. 154 (1985) 417.

[21] T.E. Jackman, K. Griffiths, W. N. Unertl, J.A. Davies, K.H. Gurtler, D.A. Harrington and P.R. Norton, Surface Sci. 179 (1987) 297.

[22] M. Fallavier, M.Y. Chartoire and J.P. Thomas, Nucl. Instr. and Meth. B15 (1986) 712.

[23] M. Fallavier, B. Hjörvarsson, M. Benmansour and J.P. Thomas, Nucl. Instr. and Meth. B64 (1992) 83.

[24] H.A. Atli, M. Alnot, J.J. Ehrhardt, J.C. Bertolini and M. Abon, Surface Sci. 269-270 (1992) 365.

[25] P. Novacek and P. Varga, Surface Sci. 248 (1991) 183.

[26] G. Amsel, C. Cohen and B. Maurel, Nucl. Instr. and Meth. B14 (1986) 226.

[27] Y. Iwata, Nucl. Instr. and Meth. B56/57 (1991) 469.

[28] J.L. Falconer and J.A. Schwarz, Catal. Rev. - Sci. Eng. 25 (1983) 141.

[29] P.A. Redhead, Vacuum 12 (1962) 203.

[30] D.A. King, Surface Sci. 47 (1975) 384.

[31] F.M. Lord and J.S. Kittelberger, Surface Sci. 43 (1974) 173.

[32] N.J. Di Nardo and E.W. Plummer, Surface Sci. 150 (1985) 89.

[33] K. Christmann and G. Ertl, in "Catalyst Characterization Science", ACS symposium Series 288, Washington DC (1985), 222

[34] W. Reimer, V. Penka, M. Skottke, R. J. Behm, G. Ertl, and W. Moritz, Surface Sci. 186 (1987) 45.

FIGURE CAPTIONS.

1) A selection of isobars. The lines are guidance to the eye. The error bar in the figure refers to the accuracy of the determination. The precision is few percent of the measured value. One monolayer corresponds to 1.01 10^{15} atoms/cm^2

2) A selection of isotherms. The lines are guidance to the eye. The error in the determination is treated in figure text 1.

3) Isosteric heat of adsorption for hydrogen on the PtNi (110) surface as a function of the coverage.

4) (A) Series of TPD spectra for different hydrogen exposures, at hydrogen pressure of 1.2 10^{-8} mbar. The temperature of the sample during adsorption was 120 K, and the heating rate was approximately 10 K/s. The exposures are given in the figure.
(B) Decomposition of the TPD spectrum (f) into three peaks α_1, α_2 and α_3.

5) Variation of the total hydrogen coverage (ML) and of the partial coverages relative to the α_1, α_2 and α_3 TPD peaks (see Fig. 4-B) as a function of the exposure.

6) Variation of the relative sticking coefficient S/S_0 on PtNi (110) at 120 K with coverage. The line is a guidance to the eye.

7) Work function changes as a function of hydrogen coverage. The coverage is obtained by using the NRA results for scaling from pressure to coverage. The hatched area is deduced from the low pressure work function measurements.

8) Schematic description of the alloy surface (following table 1) showing possible adsorption sites as discussed in the text.
I: Ni-Ni-Pt , II: Ni-Ni-Ni , III: Ni-Pt-Pt, IV: vacancies.

Table caption.

C^i_{Pt} and C^i_v are the platinum and the vacancy concentration of the ith atomic layer, the surface layer is denoted by 1. Data are from reference [10].

Table 1.

$C^1_{Pt} = 0^{+5}_{-0}$ at.% , and $C^1_v = 3^{+7}_{-3}$ at.%

$C^2_{Pt} = 95 \pm 4$ at.%

$C^3_{Pt} = 17 \pm 7$ at.%

$C^4_{Pt} = 48 \pm 13$ at.%

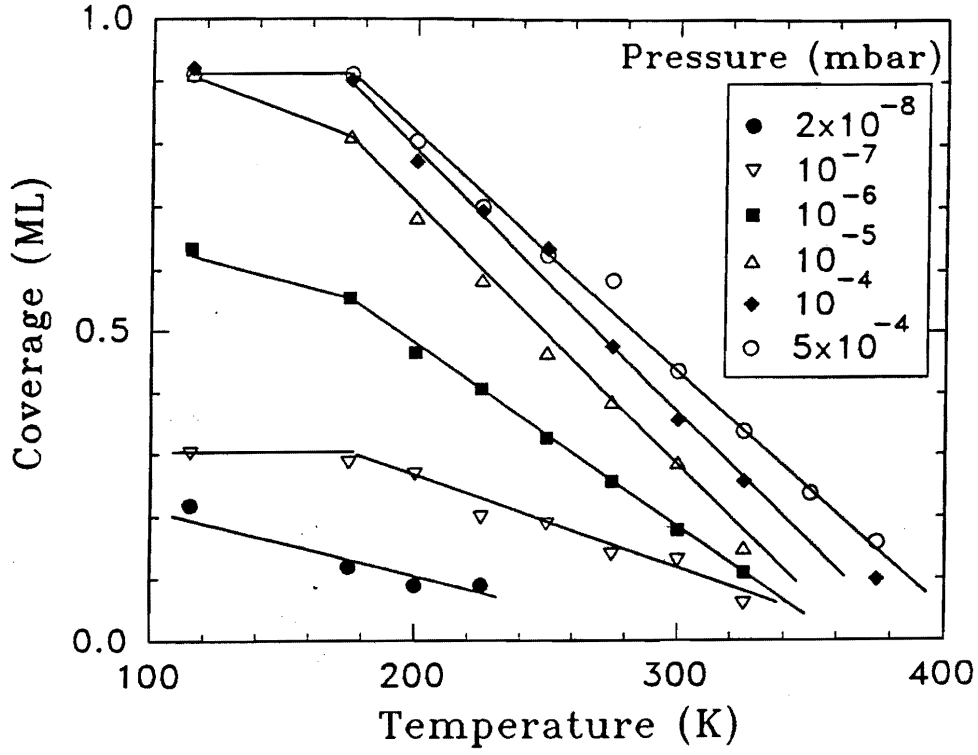

FIGURE 1

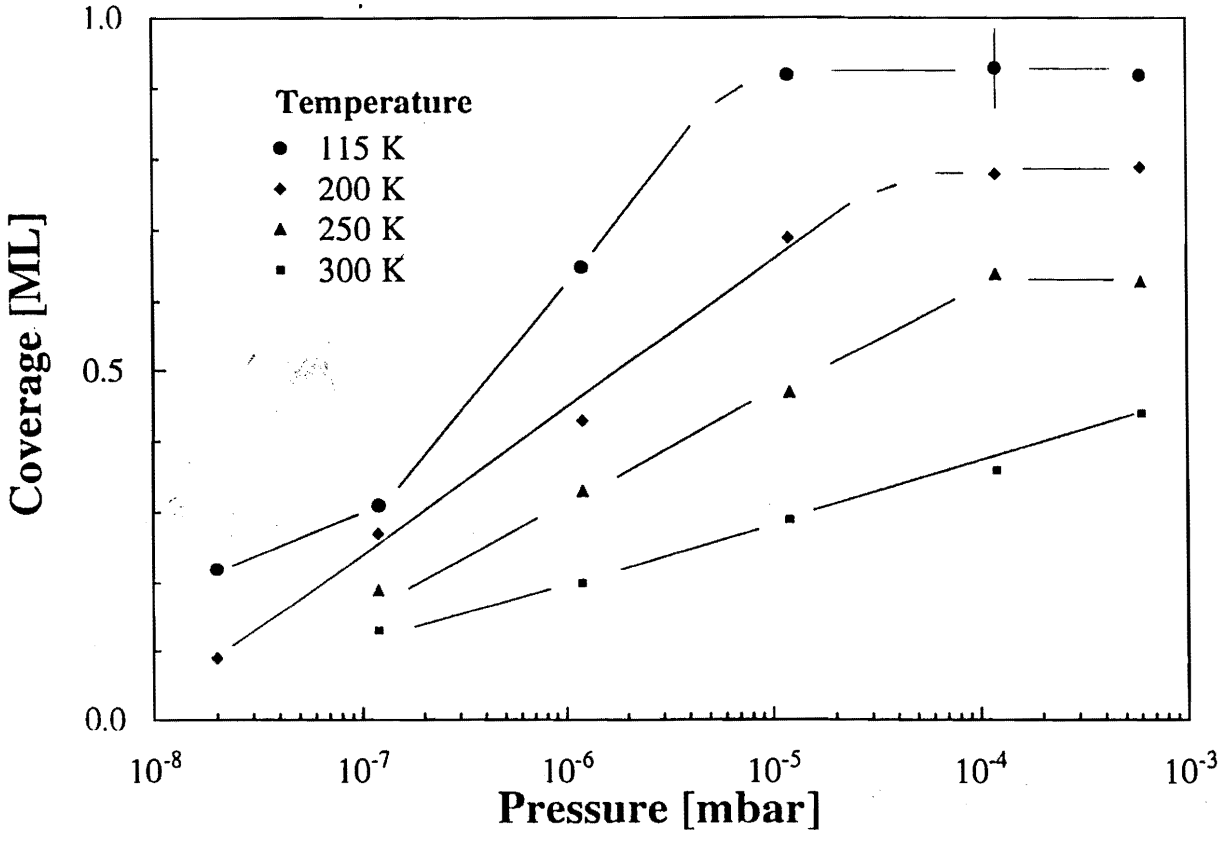

FIGURE 2

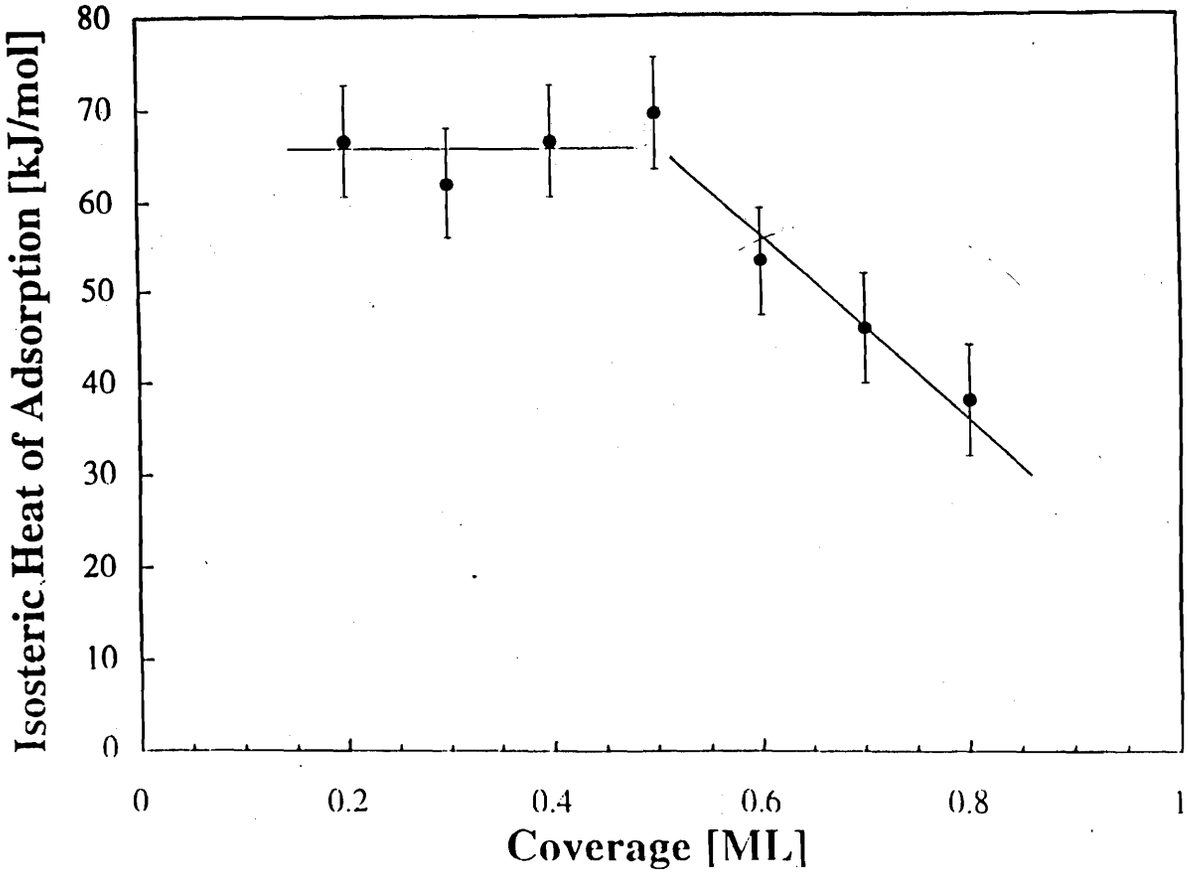

FIGURE 3

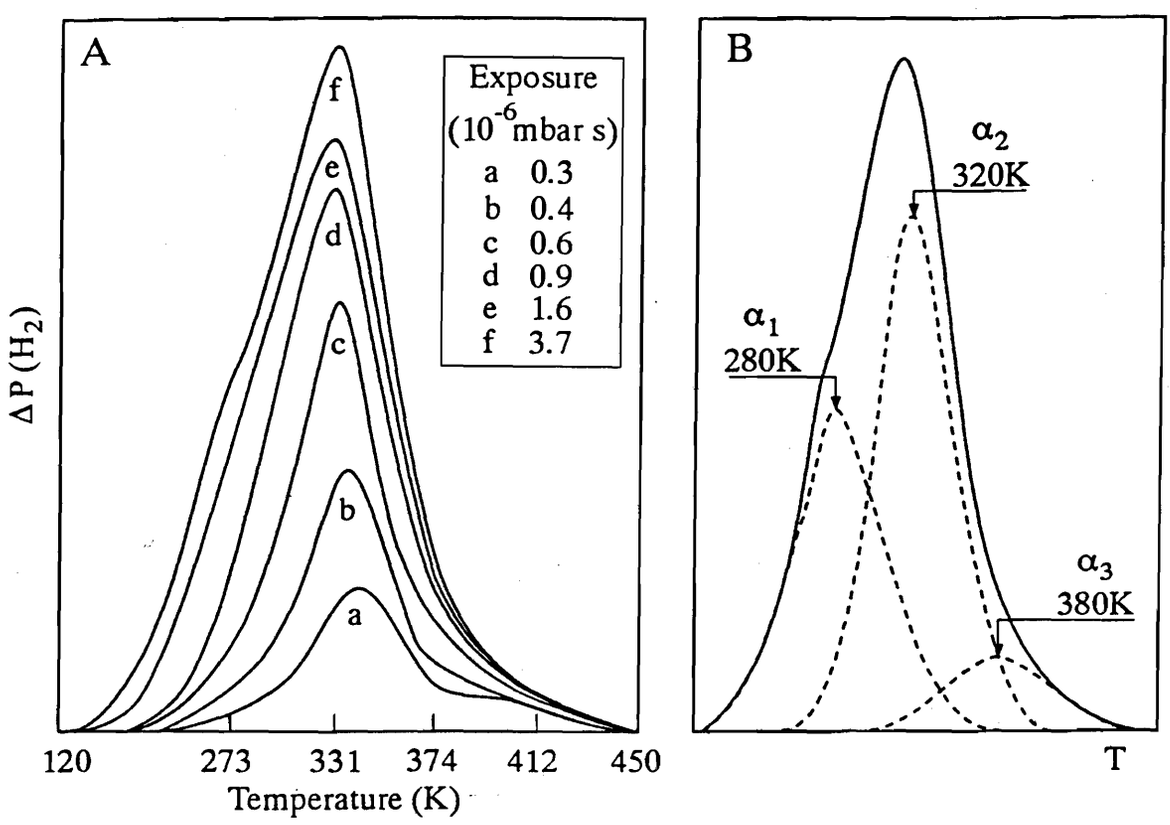

FIGURE 4

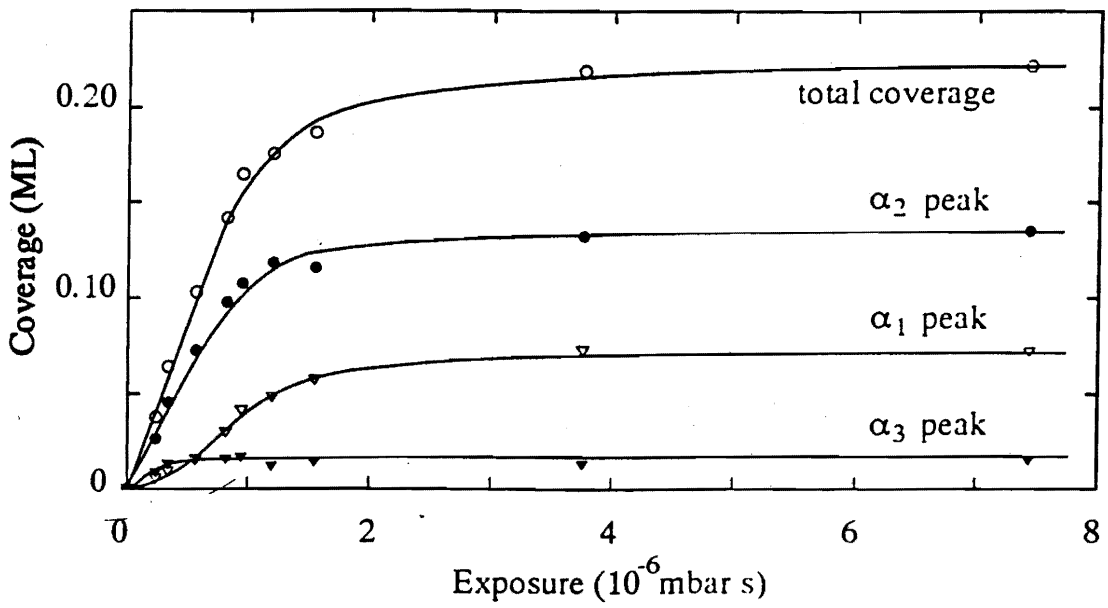

FIGURE 5

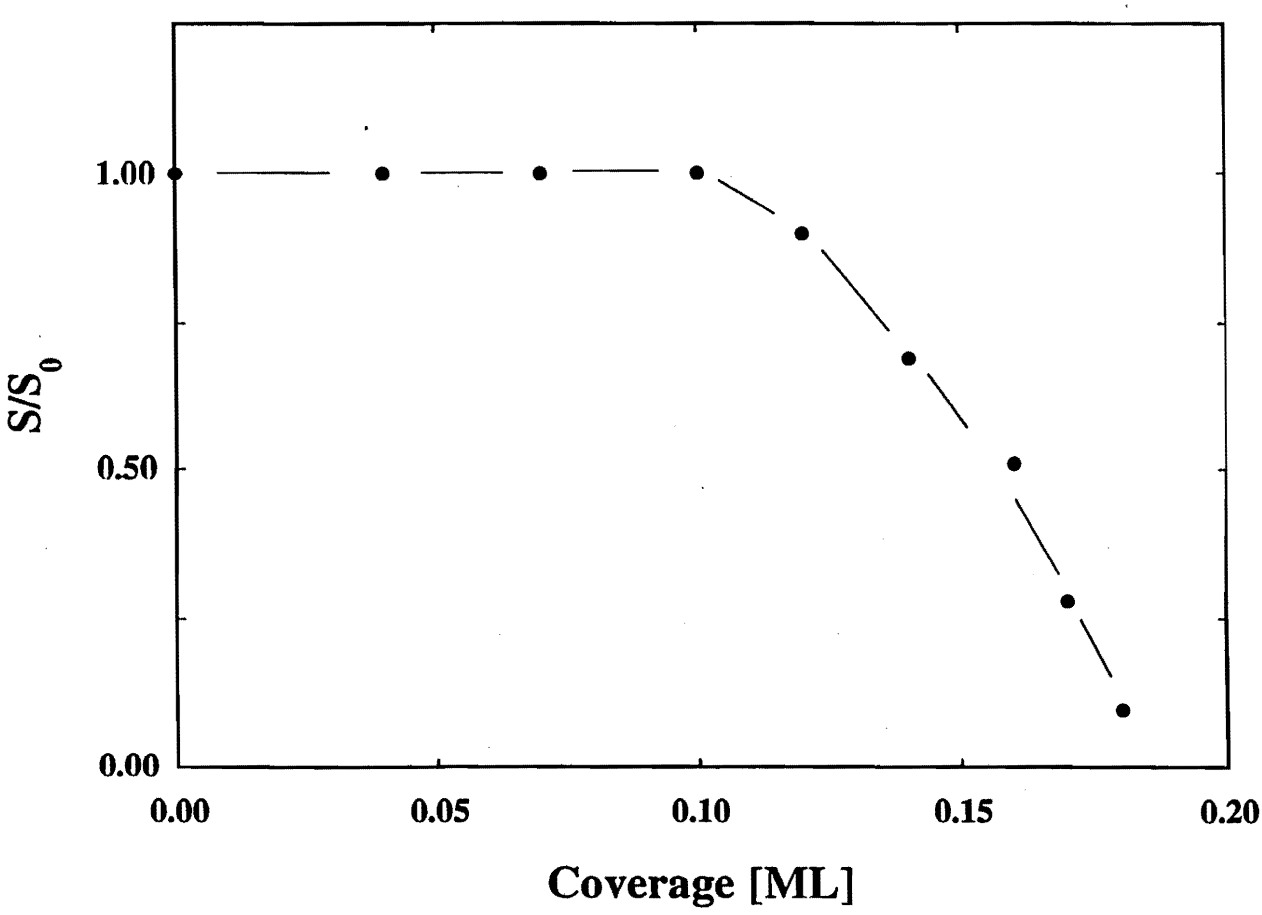

FIGURE 6

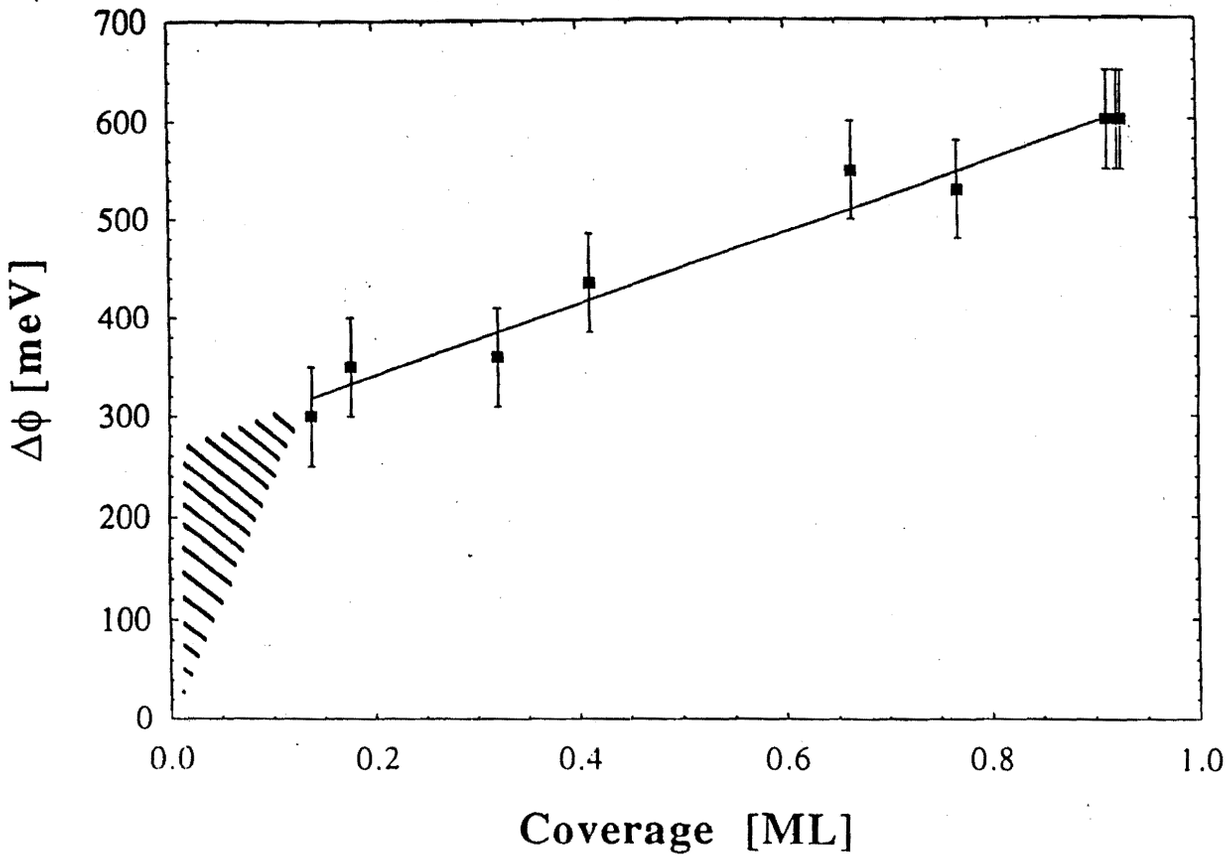

FIGURE 7

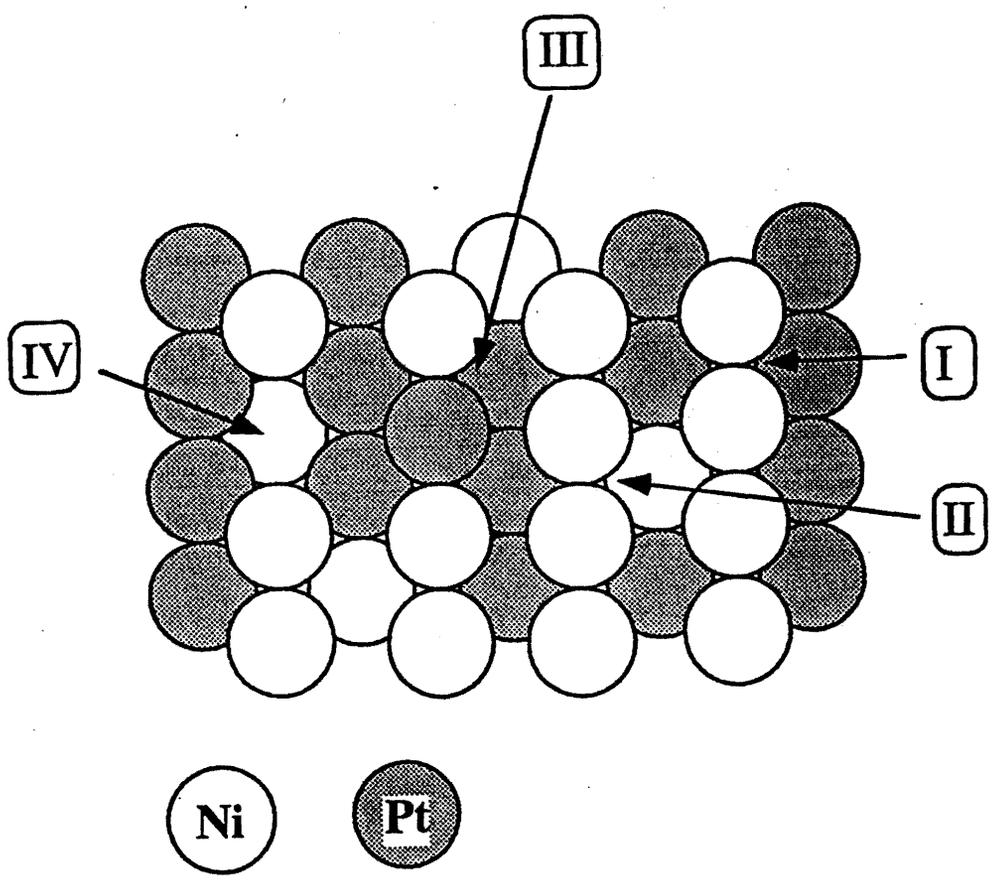

FIGURE 8